Electronic Research Archive

https://www.aimspress.com/journal/era

ERA, 33(9): 5776–5793.
DOI: 10.3934/era.2025257
Received: 17 August 2025
Revised: 11 September 2025
Accepted: 17 September 2025
Published: 26 September 2025

Research article

Efficient Jacobi-Galerkin spectral and second-order time discretization scheme for ground and first excited states of nonlinear fractional Schrödinger equation

Xiaozhuang Ma[1], Yiduo Zhang[2], Lizhen Chen[1,*] and Xiaofeng Yang[3]

[1] Beijing Computational Science Research Center, Beijing 100193, China

[2] Harrow International School, Hong Kong, China

[3] Department of Mathematics, University of South Carolina, Columbia, SC 29208, USA

* **Correspondence:** Email: lzchen@csrc.ac.cn.

Abstract: In this work, we propose an efficient and accurate numerical scheme for computing both the ground and first excited states of the nonlinear fractional Schrödinger eigenvalue problem. The method is based on a fractional gradient flow with discrete normalization, reformulated via the invariant energy quadratization (IEQ) approach to handle the nonlinear term in a linear way. Temporal discretization is performed using a second-order Crank-Nicolson scheme, while spatial discretization employs a Jacobi-Galerkin spectral method, yielding spectral convergence in space. We rigorously prove the discrete energy-decay property with respect to a modified energy functional. The resulting fully discrete scheme can compute different states simply by varying the initial condition, without altering the algorithmic framework. Numerical experiments confirm its high accuracy, efficiency, and robustness, and demonstrate its capability to capture intricate solution structures across a wide range of fractional orders and nonlinear interaction strengths.

Keywords: fractional Schrödinger; eigenvalue; IEQ; time-discrete scheme; Jacobi-Galerkin; spectral method

1. Introduction

The nonlinear Schrödinger equation (NLSE) is a fundamental nonlinear partial differential equation with a extensively spectrum of applications, including quantum mechanics [1], fluid dynamics [2], plasma physics [3], Bose-Einstein condensation [3], and nonlinear optics [4]. Owing to its remarkable versatility, it serves as a cornerstone in modeling a wide variety of nonlinear wave phenomena in both classical and quantum settings, ranging from the propagation of optical pulses in fibers, to the

dynamics of deep-water waves, and to the description of macroscopic quantum states in superfluids and condensates. The NLSE extends the classical linear Schrödinger equation by incorporating weak nonlinear effects of either quantum or classical origin, thereby enabling the modeling of self-interaction mechanisms, amplitude-dependent phase shifts, soliton formation, and modulational instabilities. These nonlinearities often arise from the interaction of the wave field with the medium, leading to feedback effects that are absent in purely linear theories. In many physical settings, the nonlinearity takes the form of a cubic (Kerr-type) term, which captures the leading-order self-phase modulation, although higher-order, saturable, or nonlocal nonlinearities may also appear in specialized contexts such as high-intensity laser propagation, dipolar Bose-Einstein condensates, or nonlocal optical media.

The specific form of the NLSE may vary depending on the physical model under consideration, with one of the most commonly studied versions given by

$$i\partial_t\phi(\mathbf{x},t) = (D_{\mathbf{x}} + V(\mathbf{x}) + \beta|\phi(\mathbf{x},t)|^2)\phi(\mathbf{x},t), \quad \mathbf{x} \in \Omega \subseteq \mathbb{R}^d, \tag{1.1}$$

where $\phi(\mathbf{x},t)$ is a complex-valued function representing the wave function or the amplitude of wave modulation, $i = \sqrt{-1}$ denotes the imaginary unit, and $V(\mathbf{x})$ denotes the potential. The parameter β describes the intensity of local (or short-range) interactions between particles, and in this context, we focus on the case where $\beta \geq 0$ (indicating repulsive interactions). Let $\Omega = (-L, L)^d$ with $d = 1, 2$ be the bounded domain. This equation poses significant challenges for finding exact solutions to practical problems. However, researchers have devised numerous analytical and numerical techniques to study its solutions, including perturbation theory, variational methods, numerical simulations, and inverse scattering methods, each offering unique insights into the behavior of nonlinear waves.

Building upon the classical Schrödinger equation of integer order, Laskin [5, 6] introduced the fractional Schrödinger equation by extending the Feynman path integral to the Lévy integral. This formulation generalizes the traditional model to incorporate fractional-order derivatives, thereby capturing a wider range of quantum dynamical behaviors. In its dimensionless form, the nonlinear fractional Schrödinger equation (NFSE, for short) is given by

$$i\partial_t\phi(\mathbf{x},t) = (D^\alpha_{\mathbf{x}} + V(\mathbf{x}) + \beta|\phi(\mathbf{x},t)|^2)\phi(\mathbf{x},t), \quad \mathbf{x} \in \Omega \subseteq \mathbb{R}^d, \tag{1.2}$$

where α represents the fractional derivative order and $D^\alpha_{\mathbf{x}}$ is the Riesz fractional operator, defined via the pseudo-differential form

$$D^\alpha_{\mathbf{x}}\phi = \mathcal{F}^{-1}\Big(\sum_{j=1}^{d} |k_j|^\alpha (\mathcal{F}\phi)(\mathbf{k})\Big), \quad \mathbf{x}, \mathbf{k} \in \mathbb{R}^d, \quad \alpha \in (0, 2], \tag{1.3}$$

where $\mathcal{F}g(k) = \displaystyle\int_{\mathbb{R}} g(x)e^{-ikx}dx$, $x, k \in \mathbb{R}$ denotes the Fourier transform of a function $g(x)$, and $\mathcal{F}^{-1}$ denotes the Fourier inverse transform. Here, $\mathbf{k} = (k_1, k_2)$ and $d = 1, 2$ (extensions to higher dimensions are also possible).

The Riesz fractional operator is equivalent to the fractional Laplacian operator $-(-\Delta)^{\alpha/2}$ [7–9] in the one-dimensional (1D) setting and under the homogeneous Dirichlet boundary conditions

$$-(-\Delta)^{\alpha/2}\phi(x) = -C_{1,\alpha}\int_{\mathbb{R}} \frac{\phi(x) - \phi(y)}{|x - y|^{1+\alpha}}dy, \quad x \in \mathbb{R}, \quad \alpha \in (0, 2], \tag{1.4}$$

where $C_{1,\alpha}$ is a normalization constant given by

$$C_{1,\alpha} = \frac{2^{\alpha-1}\alpha\Gamma((1+\alpha)/2)}{\sqrt{\pi}\Gamma(1-\alpha/2)} = \frac{\Gamma(1+\alpha)\sin(\alpha\pi/2)}{\pi}, \qquad \alpha \in (0,2]. \tag{1.5}$$

However, in two or higher dimensions, these operators defined in (1.3) and (1.4) are generally not equivalent.

To compute the stationary states of (1.2), we employ the following ansatz:

$$\phi(\mathbf{x},t) = e^{-i\lambda t}\psi(\mathbf{x}), \quad \mathbf{x} \in \Omega \subseteq \mathbb{R}^d, \tag{1.6}$$

where $\lambda \in \mathbb{R}$ is the eigenvalue and $\phi(\mathbf{x})$ is the corresponding time-independent wave function. Substituting (1.6) into (1.2) and imposing the relevant conditions yields the nonlinear fractional Schrödinger eigenvalue problem: Find $\psi(\mathbf{x})$ and $\lambda \in \mathbb{R}$ such that

$$\begin{aligned} &(D_{\mathbf{x}}^{\alpha} + V(\mathbf{x}) + \beta|\psi(\mathbf{x})|^2)\psi(\mathbf{x}) = \lambda\psi(\mathbf{x}), \quad \mathbf{x} \in \Omega \subseteq \mathbb{R}^d, \\ &\psi(\mathbf{x}) = 0, \quad \mathbf{x} \in \Omega^c = \mathbb{R}^d/\Omega, \end{aligned} \tag{1.7}$$

subject to the normalization constraint

$$\|\psi\|^2 := \int_{\Omega} |\psi(\mathbf{x})|^2 d\mathbf{x} = 1, \tag{1.8}$$

where $\psi(\mathbf{x})$ represents a real-valued eigenfunction, and $V(x)$ is taken to be either a real-valued harmonic trapping potential that reads as

$$V(\mathbf{x}) = \begin{cases} \frac{1}{2}\gamma_x^2 x^2, & d = 1, \\ \frac{1}{2}\left(\gamma_x^2 x^2 + \gamma_y^2 y^2\right), & d = 2, \end{cases} \tag{1.9}$$

or, alternatively, a combination of a harmonic potential and an optical lattice potential

$$V(\mathbf{x}) = \begin{cases} \frac{1}{2}\gamma_x^2 x^2 + \eta_x(\sin^2(\pi x)), & d = 1, \\ \frac{1}{2}\left(\gamma_x^2 x^2 + \gamma_y^2 y^2\right) + \eta_y(\sin^2(\pi x) + \sin^2(\pi y)), & d = 2. \end{cases} \tag{1.10}$$

Then, for the constrained NFSE given by (1.7) and (1.8), the free energy $E_\beta(\psi)$ and the associated eigenvalue λ corresponding to an eigenfunction $\psi(\mathbf{x})$ can be expressed as

$$E_\beta(\psi) := \int_{\Omega} \left(\left|D_{\mathbf{x}}^{\frac{\alpha}{2}}\psi(\mathbf{x})\right|^2 + V(\mathbf{x})|\psi(\mathbf{x})|^2 + \frac{\beta}{2}|\psi(\mathbf{x})|^4\right)d\mathbf{x}, \tag{1.11}$$

and

$$\begin{aligned} \lambda(\psi) &:= \int_{\Omega} \left(\left|D_{\mathbf{x}}^{\frac{\alpha}{2}}\psi(\mathbf{x})\right|^2 + V(\mathbf{x})|\psi(\mathbf{x})|^2 + \beta|\psi(\mathbf{x})|^4\right)d\mathbf{x} \\ &= E_\beta(\psi) + \frac{\beta}{2}\int_{\Omega} |\psi(\mathbf{x})|^4 d\mathbf{x}. \end{aligned} \tag{1.12}$$

In recent years, the computation and analysis of eigenvalues and eigenfunctions for the fractional Schrödinger eigenvalue problem have attracted considerable attention in the field of computational mathematics. On the theoretical side, various results have been established. For instance, [10] provided

estimates for the first eigenvalues of the fractional Laplacian in a spherical domain. Dyda et al. [11] derived bilateral bounds for the eigenvalues of the fractional Laplace operator in the unit sphere under Dirichlet boundary conditions. In their work, the classical Rayleigh-Ritz variational method was employed to obtain upper bounds, while the lower bounds were obtained using the less commonly known Aronszajn method. In [12], an explicit upper bound formula for the eigenvalue gap of a general Schrödinger operator was presented. The isoperimetric parts of the theorems in that work demonstrate that the bounds are sharp for the fundamental eigenvalue gap, as well as for infinitely many other eigenvalue gaps. A Weyl-type asymptotic formula for the eigenvalues of the fractional Laplace operator on the interval $(-1, 1)$, along with accurate bounds for the first few eigenvalues, was provided in [13]. In [14], the eigenvalue problem of the Laplace operator, with and without a potential term, was studied in bounded domains. Furthermore, an estimate of the gap between the first two eigenvalues of the Schrödinger operator was established in [15].

Complementing these theoretical developments, numerous efficient numerical methods have been proposed to compute the eigenvalues and eigenfunctions of fractional Schrödinger-type problems. Early work, such as [16], investigated both the ground and excited states of the one-dimensional linear and nonlinear fractional Schrödinger equation in an infinite potential well using finite difference discretizations. Subsequent studies expanded the range of numerical strategies. For instance, [17] proposed a finite element approximation for fractional eigenvalue problems and provided a detailed convergence analysis. High-accuracy spectral approaches have also been widely explored: In [18], the Galerkin spectral method was employed to compute eigenvalues of Riesz fractional partial differential equations with homogeneous Dirichlet boundary conditions, while [19] utilized a Fourier–Legendre–Galerkin framework for PDEs with a local fractional Laplacian, focusing on fundamental gap computations. Building on these ideas, [20] developed a Jacobi-based method for evaluating eigenvalue gaps and their statistical distributions in fractional Schrödinger problems. Other problem settings have also been addressed, including the Schrödinger-Poisson system treated by a two-grid centered difference scheme in [21], and the computation of two distinct states of the fractional Schrödinger operator using a Jacobi spectral scheme in [22]. More recent developments include the efficient spectral algorithms in [23] for eigenvalue problems involving the integral fractional Laplacian on high-dimensional balls, and the pseudo-spectral computations in [24] for stationary states and dynamics of space-fractional Schrödinger-Pitaevskii equations. In addition to these traditional numerical techniques, advanced machine learning approaches have emerged: For example, [25] introduced a neural-network-based framework capable of computing the first thirty eigenvalues for a variety of fractional Schrödinger operators.

While a variety of numerical methods have been developed for fractional Schrödinger-type eigenvalue problems, most existing approaches either involve intricate nonlinear solvers, offer only limited spatial accuracy, or require elaborate arguments to establish energy stability particularly for nonlinear cases and for computing excited states. To address these limitations, we propose a unified and fully linear numerical framework for the nonlinear fractional Schrödinger eigenvalue problem, formulated within a fractional gradient flow with discrete normalization. Motivated by [16, 26], the scheme employs a Jacobi-Galerkin spectral discretization in space, achieving exponential convergence, and a second-order Crank-Nicolson time integration based on the IEQ approach [27–29], which enables a concise and rigorous proof of the discrete energy-decaying property. This fully discrete method can compute both ground and first excited states within the same algorithm, simply by selecting different

initial conditions, without modifying the discretization or stability analysis. Compared with traditional semi-implicit Euler or fully nonlinear methods, the proposed approach delivers higher efficiency, improved spatial accuracy, and a cleaner theoretical foundation for energy stability.

The remainder of this paper is organized as follows. Section 2 introduces a fractional gradient flow with normalization for the nonlinear fractional Schrödinger eigenvalue problem, followed by its reformulation via the IEQ method. The corresponding time discretization is then presented, and the energy dissipation law is subsequently established. Section 3 describes the Jacobi-Galerkin spectral scheme employed to compute both the ground and first excited states of the fractional Schrödinger eigenvalue problem. Section 4 provides numerical experiments illustrating the accuracy and efficiency of the proposed approach for these two states. Finally, Section 5 concludes the paper with a summary and discussion of potential future research directions.

2. Fractional gradient flow and its temporal discretization

In this section, we introduce a fractional gradient flow formulation for the nonlinear fractional Schrödinger eigenvalue problem, aimed at computing both the ground and first excited states, which is then reformulated via the IEQ method. Based on this formulation, we design an efficient time-discrete scheme and rigorously establish its corresponding energy-decay property under the modified energy.

2.1. Fractional gradient flow

Define the discrete time step as $\Delta t = \frac{T}{K} > 0$, with $t \in [0, T]$ and $t_n = n\Delta t$ for $n = 0, 1, 2, \ldots, K$. Analogous to the classical case, the fractional gradient flow can be viewed as a steepest-descent evolution for the energy functional $E_\beta(u)$ without constraints, followed by a projection of the solution onto the unit sphere at the end of each time interval so as to satisfy constraint (1.8). Accordingly, the discrete normalized fractional gradient flow for the NFSE can be formulated as follows:

$$\psi_t = -\left(D_{\mathbf{x}}^{\alpha} + V(\mathbf{x}) + \beta|\psi|^2\right)\psi, \quad \mathbf{x} \in \Omega \subseteq \mathbb{R}^d, \ t \in (t_n, t_{n+1}), \tag{2.1}$$

$$\psi(\mathbf{x}, t_{n+1}) := \psi(\mathbf{x}, t_{n+1}^+) = \frac{\psi(\mathbf{x}, t_{n+1}^-)}{\|\psi(\mathbf{x}, t_{n+1}^-)\|}, \quad \mathbf{x} \in \Omega \subseteq \mathbb{R}^d, \ n \geq 0, \tag{2.2}$$

$$\psi(\mathbf{x}, t) = 0, \quad \mathbf{x} \in \Omega^c, \ t \in [0, T], \quad \psi(\mathbf{x}, 0) = \psi_0(\mathbf{x}), \ \mathbf{x} \in \Omega, \tag{2.3}$$

where $\psi(\mathbf{x}, t_{n+1}^{\pm}) = \lim_{t \to t_n^{\pm}} \psi(\mathbf{x}, t)$ and $\|\psi_0\| = 1$.

From a numerical perspective, the fractional gradient flow defined in (2.1) can be solved using standard time-stepping methods, with normalization readily enforced via a projection step at the end of each time interval.

Specifically, we set

$$\widetilde{\psi}(\cdot, t) = \frac{\psi(\cdot, t)}{\|\psi(\cdot, t)\|}, \quad t \in [0, T]. \tag{2.4}$$

For the classical case with integer derivative $\alpha = 2$, the energy-decay property of both the normalized gradient flow and its discrete counterpart were established in [26]. Following the same idea, we extend the analysis to the fractional setting and verify that the same property holds in the following theorem.

Theorem 2.1. *Assume that* $V(\mathbf{x}) \geq 0$, $\forall \mathbf{x} \in \Omega$, $\beta \geq 0$, *and* $\|\psi_0\| = 1$. *Then:*

(i) $\|\psi(\cdot, t)\| \leq \|\psi(\cdot, 0)\| = 1, \qquad t_n \leq t \leq t_{n+1},\ n \geq 0.$

(ii) *For* $\beta \geq 0$,

$$E_\beta(\psi(\cdot, t)) \leq E_\beta(\psi(\cdot, t')), \qquad t_n \leq t' \leq t \leq t_{n+1},\ n \geq 0. \tag{2.5}$$

(iii) *For* $\beta = 0$,

$$E_0(\widetilde{\psi}(\cdot, t)) \leq E_0(\widetilde{\psi}(\cdot, 0)), \qquad t_n \leq t \leq t_{n+1},\ n \geq 0. \tag{2.6}$$

Proof. (i) Multiplying ψ on both sides of Eq (2.1) and integrating over Ω yields

$$\int_\Omega \psi \cdot \psi_t d\mathbf{x} = \frac{1}{2}\frac{d}{dt}\int_\Omega \psi^2 d\mathbf{x} = -\int_\Omega \left(D_{\mathbf{x}}^\alpha \psi \cdot \psi + V(\mathbf{x})\psi^2 + \beta|\psi|^2 \cdot \psi^2\right) d\mathbf{x}.$$

Using the property of the fractional operator [30, 31], we obtain

$$\frac{1}{2}\frac{d}{dt}\|\psi\|^2 = -\int_\Omega \left(\left|D_{\mathbf{x}}^{\frac{\alpha}{2}}\psi\right|^2 + V(\mathbf{x})\left|\psi\right|^2 + \beta\left|\psi\right|^4\right) d\mathbf{x} \leq 0, \quad t_n \leq t \leq t_{n+1},\ n \geq 0,$$

which implies (i).

(ii) Similarly, by the property of the fractional operator, we have

$$\begin{aligned} \frac{d}{dt}E_\beta(\psi) &= 2\int_\Omega \left(D_{\mathbf{x}}^{\frac{\alpha}{2}}\psi \cdot D_{\mathbf{x}}^{\frac{\alpha}{2}}\psi_t + V(\mathbf{x})\psi \cdot \psi_t + \beta|\psi|^2\psi \cdot \psi_t\right) d\mathbf{x} \\ &= 2\int_\Omega \psi_t \left(D_{\mathbf{x}}^\alpha \psi + V(\mathbf{x}) \cdot \psi + \beta|\psi|^2 \cdot \psi\right) d\mathbf{x} \\ &= -2\int_\Omega |\psi_t|^2 d\mathbf{x} \leq 0, \qquad t_n \leq t \leq t_{n+1},\ n \geq 0, \end{aligned} \tag{2.7}$$

which implies (ii) and (iii).

2.2. Reformulation and temporal discretization

To illustrate the main idea of the IEQ method, we take the normalized fractional gradient flow as an example. We introduce the auxiliary variable $q = \psi^2$ and reformulate the system as

$$\psi_t = -\left(D_{\mathbf{x}}^\alpha + V(\mathbf{x}) + \beta q\right)\psi, \quad \mathbf{x} \in \Omega \subseteq \mathbb{R}^d,\ t \in (t_n, t_{n+1}), \tag{2.8}$$

$$\psi(\mathbf{x}, t_{n+1}) := \psi(\mathbf{x}, t_{n+1}^+) = \frac{\psi(\mathbf{x}, t_{n+1}^-)}{\left\|\psi(\mathbf{x}, t_{n+1}^-)\right\|}, \quad \mathbf{x} \in \Omega \subseteq \mathbb{R}^d,\ n \geq 0, \tag{2.9}$$

$$\psi(\mathbf{x}, t) = 0, \quad \mathbf{x} \in \Omega^c,\ t \in [0, T], \quad \psi(\mathbf{x}, 0) = \psi_0(\mathbf{x}),\ \mathbf{x} \in \Omega, \tag{2.10}$$

$$q_t = 2\psi\psi_t. \tag{2.11}$$

The associated energy functional can then be reformulated as

$$E_\beta(\psi, q) := \int_\Omega \left(\left|D_{\mathbf{x}}^{\frac{\alpha}{2}}\psi(\mathbf{x})\right|^2 + V(\mathbf{x})|\psi(\mathbf{x})|^2 + \frac{\beta}{2}|q(\mathbf{x})|^2\right) d\mathbf{x}. \tag{2.12}$$

Moreover, the eigenvalue corresponding to the nonlinear fractional Schrödinger equation can be expressed as

$$\begin{aligned}\lambda(\psi, q) &:= \int_\Omega \left(\left| D_{\mathbf{x}}^{\frac{\alpha}{2}} \psi(\mathbf{x}) \right|^2 + V(\mathbf{x}) |\psi(\mathbf{x})|^2 + \beta |q(\mathbf{x})|^2 \right) d\mathbf{x} \\ &= E_\beta(\psi, q) + \frac{\beta}{2} \int_\Omega |q(\mathbf{x})|^2 d\mathbf{x},\end{aligned} \tag{2.13}$$

With the reformulated variable, the following energy stability property still holds.

Theorem 2.2. *Assume that $V(\mathbf{x}) \geq 0$, $\beta \geq 0$, and $\|\psi_0\| = 1$. Then, the solution (ψ, q) of the reformulated systems* (2.8)–(2.11) *satisfies:*

(i) $\|\psi(\cdot, t)\| \leq \|\psi(\cdot, 0)\| = 1, \qquad t_n \leq t \leq t_{n+1},\ n \geq 0.$

(ii) *For $\beta \geq 0$,*

$$E_\beta(\psi(\cdot, t), q(\cdot, t)) \leq E_\beta(\psi(\cdot, t'), q(\cdot, t')), \qquad t_n \leq t' \leq t \leq t_{n+1},\ n \geq 0. \tag{2.14}$$

Proof. (i) By multiplying (2.8) by ψ and integrating over Ω, we obtain

$$\int_\Omega \psi \cdot \psi_t d\mathbf{x} = \frac{1}{2} \frac{d}{dt} \int_\Omega \psi^2 d\mathbf{x} = - \int_\Omega \left(D_{\mathbf{x}}^\alpha \psi \cdot \psi + V(\mathbf{x}) \psi^2 + \beta q \cdot \psi^2 \right) d\mathbf{x}. \tag{2.15}$$

From (2.11), integrating from 0 to t gives $q = \psi^2$. Hence,

$$\frac{1}{2} \frac{d}{dt} \|\psi\|^2 = - \int_\Omega \left(\left| D_{\mathbf{x}}^{\frac{\alpha}{2}} \psi \right|^2 + V(\mathbf{x}) \left| \psi \right|^2 + \beta \left| q \right|^2 \right) d\mathbf{x} \leq 0, \quad t_n \leq t \leq t_{n+1},\ n \geq 0. \tag{2.16}$$

This proves the result in (i).

(ii) Differentiating $E_\beta(\psi, q)$ with respect to time yields

$$\begin{aligned}\frac{d}{dt} E_\beta(\psi, q) &= 2 \int_\Omega \left(D_{\mathbf{x}}^{\frac{\alpha}{2}} \psi \cdot D_{\mathbf{x}}^{\frac{\alpha}{2}} \psi_t + V(\mathbf{x}) \psi \cdot \psi_t + \beta q \cdot q_t \right) d\mathbf{x} \\ &= 2 \int_\Omega \left(D_{\mathbf{x}}^{\frac{\alpha}{2}} \psi \cdot D_{\mathbf{x}}^{\frac{\alpha}{2}} \psi_t + V(\mathbf{x}) \psi \cdot \psi_t + \beta q \psi \cdot \psi_t \right) d\mathbf{x} \\ &= 2 \int_\Omega \psi_t \left(D_{\mathbf{x}}^\alpha \psi + V(\mathbf{x}) \cdot \psi + \beta q \cdot \psi \right) d\mathbf{x} \\ &= -2 \int_\Omega |\psi_t|^2 d\mathbf{x} \leq 0, \qquad t_n \leq t \leq t_{n+1},\ n \geq 0.\end{aligned} \tag{2.17}$$

This proves the result in (ii).

Now we construct a time-marching scheme for systems (2.8)–(2.11). Let ψ^n denote the numerical approximation of any function $\psi(\cdot, t_n)$. Our scheme is discretized in time using a second-order scheme based on the Crank-Nicolson method, implemented in the following two steps:

- **Step 1**: Compute the ψ^{n+1} and q^{n+1} using the numerical solutions from the previous time step:

$$\frac{\psi^{n+1} - \widetilde{\psi}^n}{\Delta t} = -(D_{\mathbf{x}}^\alpha + V(\mathbf{x})) \frac{\psi^{n+1} + \widetilde{\psi}^n}{2} - \beta \frac{q^{n+1} + \widetilde{q}^n}{2} (\frac{1}{2} \psi^{n+1} + \frac{1}{2} \widetilde{\psi}^n), \tag{2.18}$$

$$\frac{q^{n+1}-\widetilde{q}^n}{\Delta t}=2(\frac{1}{2}\psi^{n+1}+\frac{1}{2}\widetilde{\psi}^n)\frac{\psi^{n+1}-\widetilde{\psi}^n}{\Delta t}, \tag{2.19}$$

$$\psi^{n+1}(\mathbf{x})=0,\mathbf{x}\in\Omega^c,\psi^0(\mathbf{x})=\psi_0(\mathbf{x}),\mathbf{x}\in\Omega. \tag{2.20}$$

- **Step 2:** Update the auxiliary variables $\widetilde{\psi}^{n+1}$ and $\widetilde{q}^{n+1}$:

$$\widetilde{\psi}^{n+1}(\mathbf{x})=\frac{\psi^{n+1}(\mathbf{x})}{\left\|\psi^{n+1}\right\|},\quad \mathbf{x}\in\Omega, \tag{2.21}$$

$$\frac{\widetilde{q}^{n+1}-\widetilde{q}^n}{\Delta t}=2(\frac{1}{2}\widetilde{\psi}^{n+1}+\frac{1}{2}\widetilde{\psi}^n)\frac{\widetilde{\psi}^{n+1}-\widetilde{\psi}^n}{\Delta t}. \tag{2.22}$$

The above scheme, incorporating normalization, preserves energy stability at the discrete level, as stated in the following theorem.

Theorem 2.3. *Assume that $V(\mathbf{x})\geq 0$ and $\beta\geq 0$. Then the following discrete energy inequality holds:*

$$\widetilde{E}_\beta(\psi^{n+1},q^{n+1})\leq\widetilde{E}_\beta(\widetilde{\psi}^n,\widetilde{q}^n), \tag{2.23}$$

where $\widetilde{E}_\beta(\psi,q)=\int_\Omega(|D_{\mathbf{x}}^{\frac{\alpha}{2}}\psi|^2+V(\mathbf{x})|\psi|^2+\frac{\beta}{2}q^2)d\mathbf{x}$.

Proof. By taking the L^2-inner product of (2.18) with $\psi^{n+1}-\widetilde{\psi}^n$, we derive

$$\begin{aligned}-\frac{\|\psi^{n+1}-\widetilde{\psi}^n\|_0^2}{\Delta t} &= \frac{\|D_{\mathbf{x}}^{\frac{\alpha}{2}}\psi^{n+1}\|_0^2-\|D_{\mathbf{x}}^{\frac{\alpha}{2}}\widetilde{\psi}^n\|_0^2}{2}+V(\mathbf{x})\frac{\|\psi^{n+1}\|_0^2-\|\widetilde{\psi}^n\|_0^2}{2}\\ &\quad+\beta(\frac{q^{n+1}+\widetilde{q}^n}{2}(\frac{1}{2}\psi^{n+1}+\frac{1}{2}\widetilde{\psi}^n),(\psi^{n+1}-\widetilde{\psi}^n)).\end{aligned} \tag{2.24}$$

By taking the L^2-inner product of (2.19) with $q^{n+1}+\widetilde{q}^n$, we obtain

$$\frac{\|q^{n+1}\|_0^2-\|\widetilde{q}^n\|_0^2}{2} = ((\frac{1}{2}\psi^{n+1}+\frac{1}{2}\widetilde{\psi}^n)(\psi^{n+1}-\widetilde{\psi}^n),(q^{n+1}+\widetilde{q}^n)).$$

By combining the above two equalities, the desired result follows, and the conclusion is thus verified.

3. Fully discrete scheme using Jacobi-Galerkin spectral method

In this section, we present the implementation of the above semi-discrete time-marching scheme, in which the spatial discretization for (1.7) is carried out using the Jacobi-Galerkin spectral method. Specifically, from (2.19), we obtain

$$q^{n+1} = \widetilde{q}^n+2(\frac{1}{2}\psi^{n+1}+\frac{1}{2}\widetilde{\psi}^n)(\psi^{n+1}-\widetilde{\psi}^n) \tag{3.1}$$

which, upon substitution into (2.18), yields

$$\begin{aligned}\frac{\psi^{n+1}-\widetilde{\psi}^n}{\Delta t} =& -(D_{\mathbf{x}}^{\alpha}+V(\mathbf{x}))\frac{\psi^{n+1}+\widetilde{\psi}^n}{2}\\ &-\beta(\widetilde{q}^n(\frac{1}{2}\psi^{n+1}+\frac{1}{2}\widetilde{\psi}^n)+(\frac{1}{2}\psi^{n+1}+\frac{1}{2}\widetilde{\psi}^n)^2(\psi^{n+1}-\widetilde{\psi}^n)).\end{aligned} \tag{3.2}$$

To efficiently solve the nonlinear system (3.2) subject to the boundary condition (2.20), we employ a fixed-point iteration method. The detailed procedure for computing the solution of (3.2) using fixed-point iteration is described as follows:

Step 1: Continuing iterating to calculate the numerical solutions ψ^{n+1} until the condition

$$\max \Big| \frac{\psi^{n+1} - \psi^{\star,n+1}}{\psi^{n+1}} \Big| \leq \varepsilon \tag{3.3}$$

is satisfied, where the symbol $(\cdot)^{\star,n+1}$ denotes the numerical solution obtained in the previous iteration, with the initial guess $\psi^{\star,1} = \psi^n$, and the parameter ε is the prescribed iteration tolerance.

The iteration step is given by

$$\begin{aligned} \frac{\psi^{n+1} - \widetilde{\psi}^n}{\Delta t} =& -(D_{\mathbf{x}}^{\alpha} + V(\mathbf{x}))\frac{\psi^{n+1} + \widetilde{\psi}^n}{2} \\ & - \beta(\overline{q}^n(\frac{1}{2}\psi^{\star,n+1} + \frac{1}{2}\widetilde{\psi}^n) + (\frac{1}{2}\psi^{\star,n+1} + \frac{1}{2}\widetilde{\psi}^n)^2(\psi^{\star,n+1} - \widetilde{\psi}^n)). \end{aligned} \tag{3.4}$$

Step 2: Using the converged solution ψ^{n+1} from Step 1, compute $(\widetilde{\psi}^{n+1}, \overline{q}^{n+1})$ as follows:

$$\begin{aligned} \widetilde{\psi}^{n+1}(\mathbf{x}) &= \frac{\psi^{n+1}(\mathbf{x})}{\left\|\psi^{n+1}\right\|}, \\ q^{n+1} &= \overline{q}^n + 2(\frac{1}{2}\psi^{n+1} + \frac{1}{2}\widetilde{\psi}^n)(\psi^{n+1} - \widetilde{\psi}^n), \\ \overline{q}^{n+1} &= q^{n+1}. \end{aligned} \tag{3.5}$$

To complete the spatial discretization, we apply the Jacobi spectral method to the semi-implicit scheme (3.4). For simplicity, we consider the reference domain $\Omega = (-1, 1)$. The semi-discrete formulation of the (3.4) can then be rewritten as follows:

$$\begin{aligned} &\Big(\frac{2}{\Delta t} + D_{\mathbf{x}}^{\alpha} + V(\mathbf{x})\Big)\psi^{n+1}(\mathbf{x}) = (\frac{2}{\Delta t} - D_{\mathbf{x}}^{\alpha} - V(\mathbf{x}))\widetilde{\psi}^n \\ &- 2\beta(\overline{q}^n(\frac{1}{2}\psi^{\star,n+1} + \frac{1}{2}\widetilde{\psi}^n) + (\frac{1}{2}\psi^{\star,n+1} + \frac{1}{2}\widetilde{\psi}^n)^2(\psi^{\star,n+1} - \widetilde{\psi}^n)), \end{aligned} \tag{3.6}$$

with the homogeneous Dirichlet boundary conditions

$$\psi^{n+1}(\mathbf{x}) = 0, \quad \mathbf{x} \in \Omega^c.$$

To implement this scheme, we define the space $H^{\frac{\alpha}{2}}(\mathbb{R})$ using the classical Fourier transform, as described in [32–34]:

$$\begin{aligned} &H^{\frac{\alpha}{2}}(\mathbb{R}) = \{v \in \mathcal{D}'(\mathbb{R}) : \|v\|_{\frac{\alpha}{2},\mathbb{R}} < \infty\}, \\ &|v|_{\frac{\alpha}{2},\mathbb{R}} = \Big(\frac{1}{2\pi}\int_{\mathbb{R}} |\xi|^{\alpha}|\hat{v}(\xi)|^2 d\xi\Big)^{\frac{1}{2}}, \\ &\|v\|_{\frac{\alpha}{2},\mathbb{R}} = \Big(\frac{1}{2\pi}\int_{\mathbb{R}} (1 + |\xi|^2)^{\frac{\alpha}{2}}|\hat{v}(\xi)|^2 d\xi\Big)^{\frac{1}{2}}, \end{aligned} \tag{3.7}$$

where $\mathcal{D}'(\mathbb{R})$ is the space of generalized functions (distribution space). Subsequently, the space $H^{\frac{\alpha}{2}}(\Lambda)$ for $\Lambda = (-1, 1)$ is obtained from $H^{\frac{\alpha}{2}}(\mathbb{R})$ by restriction and extension [32–34]:

$$\begin{aligned} &H^{\frac{\alpha}{2}}(\Lambda) = \{v = u|_{\Lambda} : u \in H^{\frac{\alpha}{2}}(\Lambda)\}, \\ &\|v\|_{\frac{\alpha}{2}} = \inf_{u\in H^{\frac{\alpha}{2}}(\mathbb{R}),u|_{\Lambda}=v} \|u\|_{\frac{\alpha}{2},\mathbb{R}}. \end{aligned} \tag{3.8}$$

Given a Banach space X with norm $\|\cdot\|_X$ and a positive constant $\alpha > 0$, we define

$$\begin{aligned} &H^{\frac{\alpha}{2}}(\Lambda, X) = \{u| \, \|u(\cdot, x)\|_X \in H^{\frac{\alpha}{2}}(\Lambda, X)\}, \\ &\|u\|_{H^{\frac{\alpha}{2}}(\Lambda,X)} = \Big\|\|u(\cdot, x)\|_X\Big\|_{\frac{\alpha}{2},\Lambda}. \end{aligned} \tag{3.9}$$

Finally, we define $H^{\frac{\alpha}{2}}(\Omega)$ and $H_0^{\frac{\alpha}{2}}(\Omega)$ as follows:

$$\begin{aligned} &H^{\frac{\alpha}{2}}(\Omega) = H^{\frac{\alpha}{2}}(\Lambda, L^2(\Lambda)) \cap L^2(\Lambda, H^{\frac{\alpha}{2}}(\Lambda)), \\ &\|u\|_{H^{\frac{\alpha}{2}}(\Omega)} = \Big(\|u\|^2_{H^{\frac{\alpha}{2}}(\Lambda,L^2(\Lambda))} + \|u\|^2_{L^2(\Lambda,H^{\frac{\alpha}{2}}(\Lambda))}\Big)^{\frac{1}{2}}, \\ &H_0^{\frac{\alpha}{2}}(\Omega) = \Big\{u \in H^{\frac{\alpha}{2}}(\Omega), u|_{\partial\Omega} = 0\Big\}. \end{aligned} \tag{3.10}$$

Using the above notations, the weak formulation of (3.6) can be stated as follows: Find $\psi^{n+1} \in H_0^{\frac{\alpha}{2}}(\Omega)$ such that, $\forall v \in H_0^{\frac{\alpha}{2}}(\Omega)$, we have

$$\begin{aligned} &\Big((\frac{2}{\Delta t} + D^{\alpha}_{\mathbf{x}} + V(\mathbf{x}))\psi^{n+1}(\mathbf{x}), v\Big) \\ =&\Big((\frac{2}{\Delta t} - D^{\alpha}_{\mathbf{x}} - V(\mathbf{x}))\widetilde{\psi}^n - 2\beta(\overline{q}^n(\frac{3}{2}\psi^{\star,n+1} - \frac{1}{2}\widetilde{\psi}^n) + (\frac{3}{2}\psi^{\star,n+1} - \frac{1}{2}\widetilde{\psi}^n)^2(\psi^{\star,n+1} - \widetilde{\psi}^n)), v\Big). \end{aligned} \tag{3.11}$$

Let $\mathcal{J}_n^{-\frac{\alpha}{2},-\frac{\alpha}{2}}(x) = (1 - x^2)^{\frac{\alpha}{2}}P_n^{\frac{\alpha}{2},\frac{\alpha}{2}}(x)$ for $\alpha > -2$ be the generalized Jacobi function, where $P_n^{\frac{\alpha}{2},\frac{\alpha}{2}}(x)$ denotes the Jacobi polynomial over the interval $(-1, 1)$. According to Theorem 2 in [35], we can derive certain properties or representations related to these generalized Jacobi functions:

$$D^{\alpha}\mathcal{J}_m^{-\frac{\alpha}{2},-\frac{\alpha}{2}}(x) = \frac{\Gamma(m + \alpha + 1)}{m!}P_m^{\frac{\alpha}{2},\frac{\alpha}{2}}(x). \tag{3.12}$$

Therefore, the following equation holds:

$$\Big(D^{\frac{\alpha}{2}}\mathcal{J}_m^{-\frac{\alpha}{2},-\frac{\alpha}{2}}(x), D^{\frac{\alpha}{2}}\mathcal{J}_n^{-\frac{\alpha}{2},-\frac{\alpha}{2}}(x)\Big) = \frac{2^{\alpha+1}\Gamma(m + \alpha/2 + 1)^2}{m!^2(2m + \alpha + 1)}\delta_{m,n}.$$

Let $\mathbb{P}_N$ denote the set of all polynomials of degree less than or equal to N. For $\alpha > 0$, we introduce the finite-dimensional fractional space $\mathbb{F}_N^{-\frac{\alpha}{2},-\frac{\alpha}{2}}(\Omega)$ as

$$\mathbb{F}_N^{-\frac{\alpha}{2},-\frac{\alpha}{2}}(\Lambda) := \text{span}\Big\{\varphi_n(x) := \frac{\sqrt{2n + \alpha + 1}n!}{2^{\alpha/2+1/2}\Gamma(n + \alpha/2 + 1)}\mathcal{J}_n^{-\frac{\alpha}{2},-\frac{\alpha}{2}}(x), \quad 0 \le n \le N\Big\}.$$

Hence, the Jacobi–Galerkin spectral method for (3.11) is stated as follows: Find $\psi_N^{n+1} \in \mathbb{F}_N^{-\frac{\alpha}{2},-\frac{\alpha}{2}}(\Omega)$ such that

$$\begin{aligned} &\Big((\frac{2}{\Delta t} + D^{\alpha}_{\mathbf{x}} + V(x))\psi_N^{n+1}(x), v_N\Big) = \Big((\frac{2}{\Delta t} - D^{\alpha}_{\mathbf{x}} - V(\mathbf{x}))\widetilde{\psi}_N^n \\ &- 2\beta(\overline{q}_N^n(\frac{1}{2}\psi_N^{\star,n+1} + \frac{1}{2}\widetilde{\psi}_N^n) + (\frac{1}{2}\psi_N^{\star,n+1} + \frac{1}{2}\widetilde{\psi}_N^n)^2(\psi_N^{\star,n+1} - \widetilde{\psi}_N^n)), v_N\Big), \quad \forall v_N \in \mathbb{F}_N^{-\frac{\alpha}{2},-\frac{\alpha}{2}}(\Omega). \end{aligned} \tag{3.13}$$

To implement the method, we first expand $\psi_N^{n+1}(x)$ in terms of the basis functions as

$$\psi_N^{n+1}(x) = \sum_{i=0}^{N} \hat{\psi}_i^{n+1} \varphi_i(x), \tag{3.14}$$

where $\varphi_i(x), i = 0, \cdots, N$ are the basis functions of $\mathbb{F}_N^{-\frac{\alpha}{2},-\frac{\alpha}{2}}(\Lambda)$. We define the following matrices and vectors:

$$\begin{aligned}
&\mathbf{M}_{ij} = (\varphi_j(x), \varphi_i(x)),\ \mathbf{S}_{ij} = (D_x^{\alpha}\varphi_j(x), \varphi_i(x)),\\
&\mathbf{V}_{ij} = (V(x)\varphi_j(x), \varphi_i(x)),\\
&\mathbf{F}_j^n = 2\beta(\widetilde{q}_N^n(\frac{3}{2}\psi_N^{\star,n+1} - \frac{1}{2}\widetilde{\psi}_N^n) + (\frac{3}{2}\psi_N^{\star,n+1} - \frac{1}{2}\widetilde{\psi}_N^n)^2(\psi_N^{\star,n+1} - \widetilde{\psi}_N^n), \varphi_j(x)),\\
&\mathbf{M} = (\mathbf{M}_{ij})_{0\le i,j\le N},\ \mathbf{S} = (\mathbf{S}_{ij})_{0\le i,j\le N},\ \mathbf{V} = (\mathbf{V}_{ij})_{0\le i,j\le N},\ \mathbf{F} = (\mathbf{F}_j)_{0\le j\le N}.
\end{aligned}$$

Substituting the expansion (3.14) into (3.13) and choosing the test functions $v_N = \varphi_j(x), j = 0, \cdots, N$, we obtain the following matrix system:

$$\Big(\frac{2\mathbf{M}}{\Delta t} + \mathbf{S} + \mathbf{V}\Big)\hat{\boldsymbol{\psi}}^{n+1} = \Big(\frac{2\mathbf{M}}{\Delta t} - \mathbf{S} - \mathbf{V}\Big)\hat{\boldsymbol{\psi}}^{n} - \mathbf{F}^n, \tag{3.15}$$

where $\hat{\boldsymbol{\psi}}^{n+1} = (\hat{\psi}_0^{n+1}, \hat{\psi}_1^{n+1}, \cdots, \hat{\psi}_N^{n+1})$ is the coefficient vector representing the numerical solution for $\psi_N^{n+1}(x)$.

It is clear that the mass matrix $\mathbf{M}$, the potential matrix $\mathbf{V}$, the stiffness matrix $\mathbf{S}$, and the nonlinear term vector $\mathbf{F}$ are all symmetric and positive definite. The explicit expressions of $\mathbf{M}$ and $\mathbf{S}$ are given in [18] as follows:

$$\begin{aligned}
&\mathbf{S}_{ij} = (D^{\alpha/2}\varphi_j, D^{\alpha/2}\varphi_i) = \delta_{ij},\\
&\mathbf{M}_{ij} = (\varphi_j, \varphi_i) = \begin{cases} \dfrac{(-1)^{\frac{j-i}{2}}\sqrt{\pi(2i+\alpha+1)(2j+\alpha+1)}\Gamma(\alpha+1)(i+j)!}{2^{\alpha+i+j+1}\Gamma(\alpha+\frac{i+j}{2}+\frac{3}{2})\Gamma(\frac{\alpha}{2}+\frac{i-j}{2}+1)\Gamma(\frac{\alpha}{2}+\frac{j-1}{2}+1)(\frac{i+j}{2})!}, & i+j \text{ even};\\ 0, & i+j \text{ odd}. \end{cases}
\end{aligned}$$

Therefore, the linear algebraic system (3.15) can be assembled and solved directly.

4. Numerical examples

In this section, we present several numerical experiments to compute the two different states of the NFSE in the one-dimensional case to validate the accuracy, efficiency, and applicability of the proposed scheme.

4.1. Accuracy test

In the subsequent simulations, we set the physical domain to $\Omega = (-1, 1)$, choose the time-step size $\Delta t = 0.001$, and use a convergence tolerance of $\varepsilon = 10^{-12}$. To evaluate the convergence rate of the proposed method, we take the eigenvalues computed with $N = 480$ as the benchmark reference. Figure 1 presents the errors of the first two eigenvalues versus the polynomial degree N for various

values of α, plotted on a logarithmic-logarithmic scale. The results indicate that the errors decrease rapidly as N increases, demonstrating the spectral accuracy of our proposed numerical method.

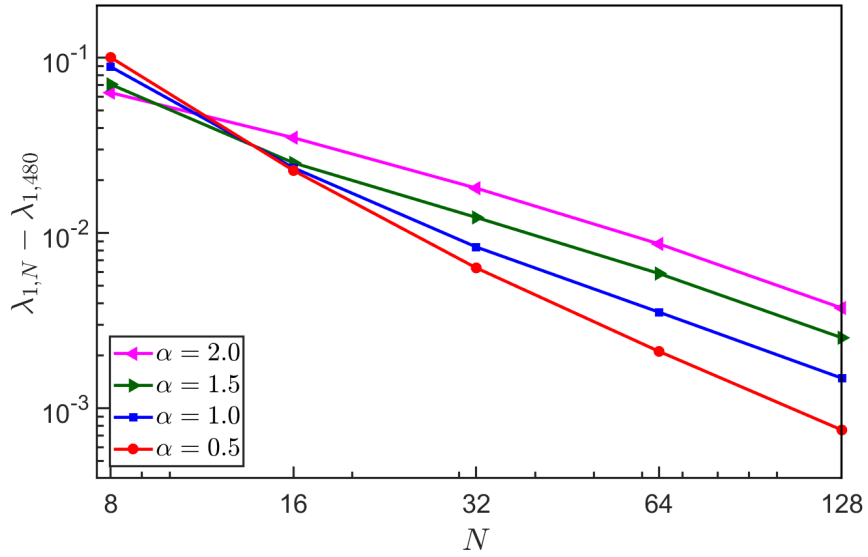

(a) $\lambda_{1,N} - \lambda_{1,480}$ in the log-log scale.

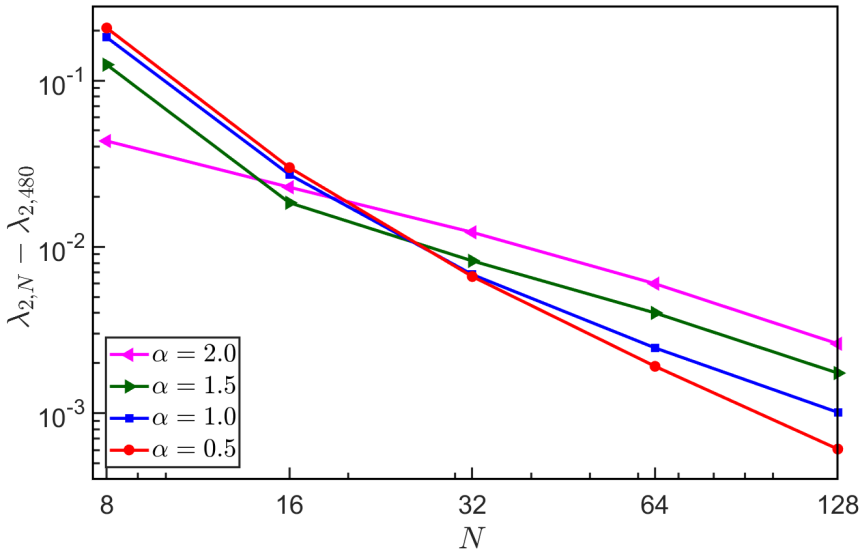

(b) $\lambda_{2,N} - \lambda_{2,480}$ in the log-log scale.

Figure 1. The errors of the eigenvalue λ_1 (left) and λ_2 (right) with various N and α in logarithm-logarithm scale, respectively.

4.2. The ground and first excited states

In quantum mechanics and related physical models, the ground state refers to the lowest-energy stationary solution of the governing equation, while the excited states correspond to stationary solutions

with higher energy levels. These states are eigenfunctions of the underlying Hamiltonian operator and are associated with discrete eigenvalues representing their energy. The ground state typically exhibits no internal nodes, whereas the m-th excited state contains exactly m internal nodes in its spatial profile.

For the NFSE, the ground state represents the most stable configuration of the system, balancing the effects of dispersion (characterized by the fractional Laplacian order α), the potential field $V(x)$, and the nonlinear interaction strength β. Excited states, on the other hand, describe higher-energy configurations that can be physically interpreted as metastable or transition states, and are important in modeling phenomena such as quantum transitions, nonlinear wave interactions, and localized modes in fractional quantum systems.

In the following numerical experiments, we consider the domain $\Omega = (-1, 1)$ and choose the initial condition

$$u(x) = \sin\left(\frac{(k+1)\pi(x+1)}{2}\right), \quad x \in \Omega,\ k = 0, 1, \tag{4.1}$$

where $k = 0$ corresponds to computing the ground state and $k = 1$ corresponds to computing the first excited state.

For one-dimensional Schrödinger-type eigenvalue problems, including the NFSE model we study in this paper, the nodal properties of the eigenfunctions follow directly from the Sturm-Liouville theory:

- The ground state (lowest-energy eigenfunction) has no internal nodes in the domain Ω, except for zeros at the boundaries due to the boundary conditions. The profile is strictly positive (or strictly negative) across Ω, with a single smooth peak at the center and monotonic decay towards the boundaries.
- The first excited state (second-lowest eigenfunction) has exactly one internal zero in Ω, typically located at the domain center $x = 0$, and changes sign across this node, producing one positive lobe and one negative lobe.

These properties give a straightforward criterion for identifying the states in numerical computations. In Figure 2 with free potential $V(x) = 0$, the panels in the left column (a), (c), and (e) display eigenfunctions that are strictly positive in $(-1, 1)$ with no sign changes, hence corresponding to the ground states $u_1^\alpha(x)$. The panels in the right column (b), (d), (f) each show a single zero crossing at $x = 0$, indicating exactly one internal node; these are the first excited states $u_2^\alpha(x)$. Physically, the ground state represents the most stable configuration of the system, minimizing the total energy, while the first excited state corresponds to the next higher energy mode, relevant to quantum transitions or metastable behavior. The insets in Figure 2 further reveal boundary layers near $x = \pm 1$, which become more pronounced when the fractional order α is small or the nonlinear interaction strength β is large, indicating sharper localization of the wave function near the boundaries.

In Figure 3, we set $V(x) = \frac{x^2}{2}$, introducing a harmonic confining potential into the NFSE. Compared with the free-potential case in Figure 2, the presence of this potential compresses the eigenfunctions toward the center of the domain, resulting in narrower spatial extent and stronger central localization. As the nonlinear interaction strength β increases, both the ground and first excited states exhibit broader plateaus in the central region and steeper gradients near the boundaries. These steep boundary layers are further amplified when the fractional order α is small, reflecting the reduced dispersive effect of the fractional Laplacian. The insets in Figure 3 clearly illustrate these boundary layer structures and their dependence on α and β, highlighting the interplay between dispersion, nonlinearity, and external confinement.

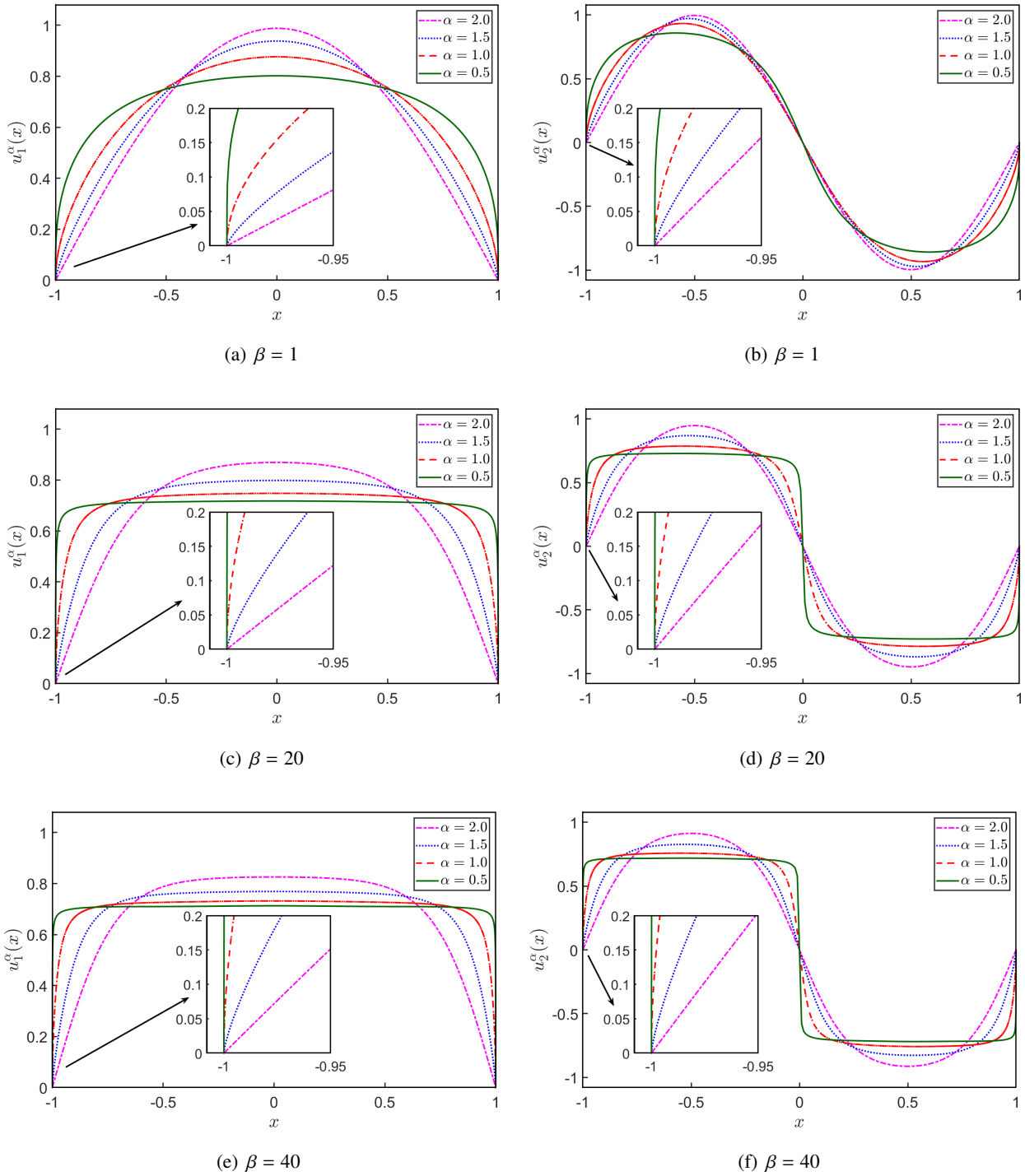

(a) $\beta = 1$ (b) $\beta = 1$

(c) $\beta = 20$ (d) $\beta = 20$

(e) $\beta = 40$ (f) $\beta = 40$

Figure 2. Ground states $u_1^\alpha(x)$ (left column) and the first excited states $u_2^\alpha(x)$ (right column) of the one-dimensional NFSE with free potential $V(x) = 0$ for various values of the fractional order α and nonlinear interaction strength β, computed by our proposed scheme.

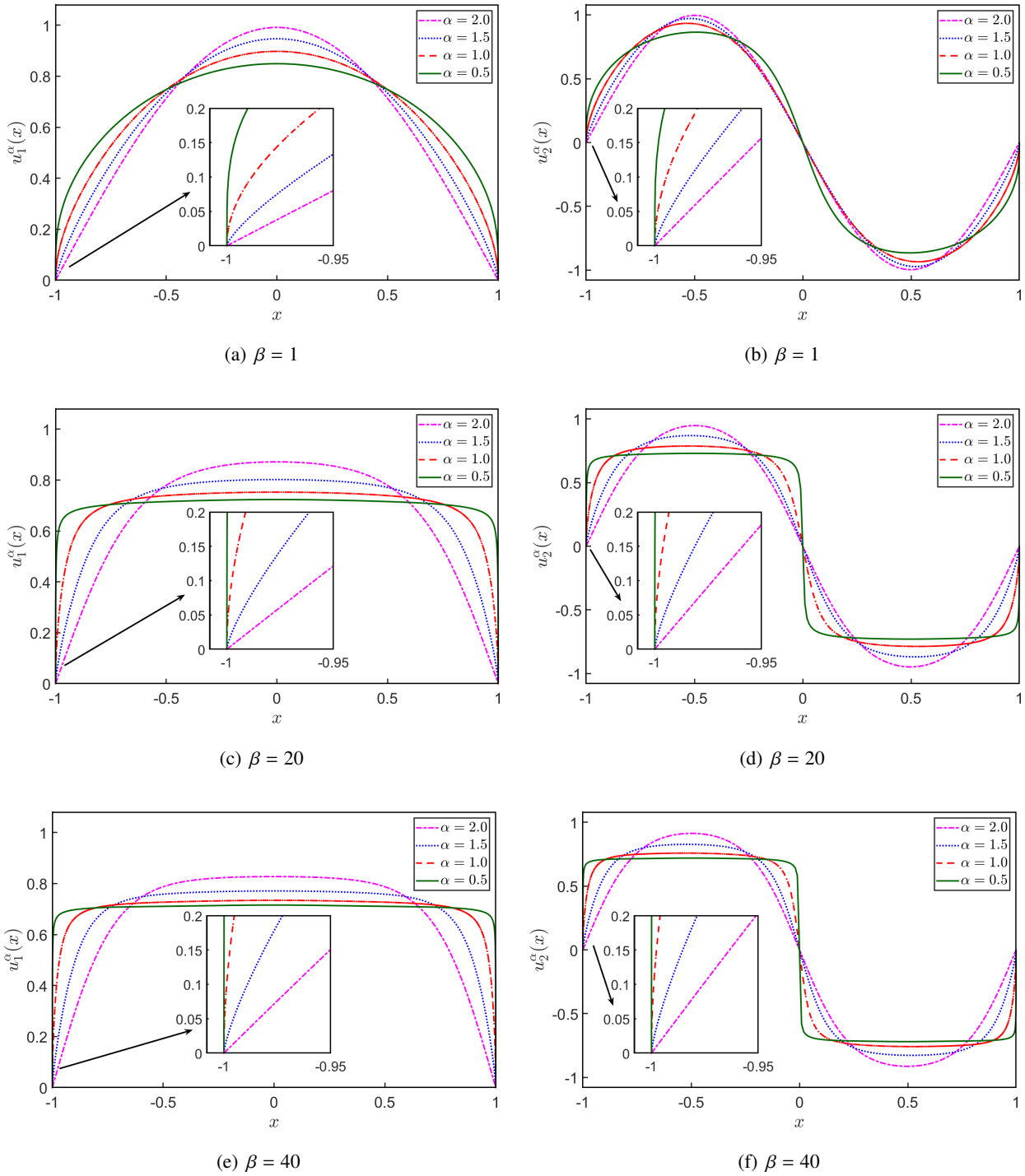

(a) $\beta = 1$ (b) $\beta = 1$

(c) $\beta = 20$ (d) $\beta = 20$

(e) $\beta = 40$ (f) $\beta = 40$

Figure 3. Ground states $u_1^\alpha(x)$ (left column) and the first excited states $u_2^\alpha(x)$ (right column) of the one-dimensional NFSE with potential $V(x) = \frac{x^2}{2}$ for various values of the fractional order α and nonlinear interaction strength β, computed by our proposed scheme.

5. Conclusions

In this work, we have developed an efficient and accurate numerical method for computing the ground state and the first excited state of the nonlinear fractional Schrödinger equation. A normalized fractional gradient flow was formulated, and the corresponding energy decay property was established under a modified energy framework. The normalized flow was then discretized in time using a second-order scheme based on the invariant energy quadratization approach, and in space using the Jacobi-Galerkin spectral method. To efficiently address the nonlinear term in the fully discrete scheme, a fixed-point iteration was employed. Several numerical experiments were carried out to compute both the ground state and the first excited state, confirming the spectral accuracy of the proposed method in the spatial domain and demonstrating its robustness for different parameter regimes. Future work will focus on extending the proposed framework to a broader class of fractional partial differential equations and exploring its applicability to higher-dimensional problems and more complex nonlinearities.

Use of AI tools declaration

The authors declare they have not used Artificial Intelligence (AI) tools in the creation of this article.

Acknowledgments

The work of Lizhen Chen would like to acknowledge the support from National Natural Science Foundation of China (Grants Nos. 12261017, 11671166 and U1530401).

Conflict of interest

The authors declare there are no conflicts of interest.

References

1. H. D. Doebner, G. A. Goldin, P. Nattermann, Gauge transformations in quantum mechanics and the unification of nonlinear schrödinger equations, *J. Math. Phys.*, **40** (1999), 49–63. https://doi.org/10.1063/1.532786
2. V. Banica, R. Lucà, N. Tzvetkov, L. Vega, Blow-up for the 1d cubic nls, *Commun. Math. Phys.*, **405** (2024), 11. https://doi.org/10.1007/s00220-023-04906-3
3. W. Bao, The nonlinear schrödinger equation and applications in bose-einstein condensation and plasma physics, in *Dynamics in Models of Coarsening, Coagulation, Condensation and Quantization*, (2007), 141–239. https://doi.org/10.1142/9789812770226_0003
4. G. Fibich, G. Papanicolaou, Self-focusing in the perturbed and unperturbed nonlinear schrödinger equation in critical dimension, *SIAM J. Appl. Math.*, **60** (1999), 183–240. https://doi.org/10.1137/S0036139997322407
5. N. Laskin, Fractional quantum mechanics, *Phys. Rev. E*, **62** (2000), 3135–3145. https://doi.org/10.1103/PhysRevE.62.3135

6. N. Laskin, Fractional schrödinger equation, *Phys. Rev. E*, **66** (2002), 056108. https://doi.org/10.1103/PhysRevE.66.056108
7. Q. Yang, I. Turner, F. Liu, M. Ilić, Novel numerical methods for solving the time-space fractional diffusion equation in two dimensions, *Comput. Phys. Commun.*, **33** (2011), 1159–1180. https://doi.org/10.1137/100800634
8. E. Di Nezza, G. Palatucci, E. Valdinoci, Hitchhiker's guide to the fractional sobolev spaces, *Bull. Sci. Math.*, **136** (2012), 521–573. https://doi.org/10.1016/j.bulsci.2011.12.004
9. A. Lischke, G. F. Pang, M. Gulian, F. Y. Song, C. Glusa, X. N. Zheng, et al., What is the fractional Laplacian? A comparative review with new results, *J. Comput. Phys.*, **404** (2020), 109009. https://doi.org/10.1016/j.jcp.2019.109009
10. B. Dyda, Fractional calculus for power functions and eigenvalues of the fractional Laplacian, *Fract. Calc. Appl. Anal.*, **15** (2012), 536–555. https://doi.org/10.2478/s13540-012-0038-8
11. B. Dyda, A. Kuznetsov, M. Kwaśnicki, Eigenvalues of the fractional laplace operator in the unit ball, *J. London Math. Soc.*, **95** (2017), 500–518. https://doi.org/10.1112/jlms.12024
12. E. M. Harrell, Commutators, eigenvalue gaps, and mean curvature in the theory of Schrödinger operators, *Commun. Partial Differ. Equations*, **32** (2007), 401–413. https://doi.org/10.1080/03605300500532889
13. M. Kwaśnicki, Eigenvalues of the fractional laplace operator in the interval, *J. Funct. Anal.*, **262** (2012), 2379–2402. https://doi.org/10.1016/j.jfa.2011.12.004
14. P. Li, S. T. Yau, On the schrödinger equation and the eigenvalue problem, *Commun. Math. Phys.*, **88** (1983), 309–318. https://doi.org/10.1007/BF01213210
15. I. M. Singer, B. Wong, S. S. T. Yau, S. T. Yau, An estimate of the gap of the first two eigenvalues in the schrödinger operator, *Ann. Sc. Norm. Super. Pisa Cl. Sci.*, **12** (1985), 319–333. Available from: https://www.numdam.org/item/?id=ASNSP_1985_4_12_2_319_0.
16. S. W. Duo, Y. Z. Zhang, Computing the ground and first excited states of the fractional schrödinger equation in an infinite potential well, *Commun. Comput. Phys.* , **18** (2015), 321–350. https://doi.org/10.4208/cicp.300414.120215a
17. J. P. Borthagaray, L. M. Del Pezzo, S. Martínez, Finite element approximation for the fractional eigenvalue problem, *J. Sci. Comput.*, **77** (2018), 308–329. https://doi.org/10.1007/s10915-018-0710-1
18. L. Z. Chen, Z. P. Mao, H. Y. Li, Jacobi-Galerkin spectral method for eigenvalue problems of riesz fractional differential equations, preprint, arXiv:1803.03556.
19. W. Z. Bao, X. R. Ruan, J. Shen, C. T. Sheng, Fundamental gaps of the fractional schrödinger operator, *Commun. Math. Sci.*, **17** (2019), 447–471. https://doi.org/10.4310/CMS.2019.v17.n2.a7
20. W. Z. Bao, L. Z. Chen, X. Y. Jiang, Y. Ma, A jacobi spectral method for computing eigenvalue gaps and their distribution statistics of the fractional schrödinger operator, *J. Comput. Phys.*, **421** (2020), 109733. https://doi.org/10.1016/j.jcp.2020.109733
21. S. L. Chang, C. S. Chien, B. W. Jeng, An efficient algorithm for the schrödinger-poisson eigenvalue problem, *J. Comput. Appl. Math.*, **205** (2007), 509–532. https://doi.org/10.1016/j.cam.2006.05.013

22. Y. Ma, L. Z. Chen, A Jacobi-Galerkin spectral method for computing the ground and first excited states of nonlinear fractional schrödinger equation, *East Asian J. Appl. Math.*, **10** (2020), 274–294. https://doi.org/10.4208/eajam.140319.180719
23. S. N. Ma, H. Y. Li, Z. M. Zhang, H. Chen, L. C. Chen, Efficient spectral methods for eigenvalue problems of the integral fractional laplacian on a ball of any dimension, *J. Comput. Math.*, **42** (2024), 1032–1062. https://doi.org/10.4208/jcm.2304-m2022-0243
24. X. Antoine, Q. L. Tang, Y. Zhang, On the ground states and dynamics of space fractional nonlinear schrödinger/gross-pitaevskii equations with rotation term and nonlocal nonlinear interactions, *J. Comput. Phys.*, **325** (2016), 74–97. https://doi.org/10.1016/j.jcp.2016.08.009
25. Y. X. Gou, P. B. Ming, A deep learning method for computing eigenvalues of the fractional schrödinger operator, *J. Syst. Sci. Complexity*, **37** (2024), 391–412. https://doi.org/10.1007/s11424-024-3250-9
26. W. Z. Bao, Q. Du, Computing the ground state solution of bose-einstein condensates by a normalized gradient flow, *SIAM J. Sci. Comput.*, **25** (2004), 1674–1697. https://doi.org/10.1137/S1064827503422956
27. Z. Xu, X. Yang, H. Zhang, Z. Xie. Efficient and linear schemes for anisotropic cahn–hilliard modeln using the stabilized-invariant energy quadratization (s-ieq) approach, *Comput. Phys. Commun.*, **238** (2019), 36–49. https://doi.org/10.1016/j.cpc.2018.12.019
28. X. Yang, Linear, first and second-order, unconditionally energy stable numerical schemes for the phase field model of homopolymer blends, *J. Comput. Phys.*, **327** (2016), 294–316. https://doi.org/10.1016/j.jcp.2016.09.029
29. X. Yang, X. He, A fully-discrete decoupled finite element method for the conserved allen–cahn type phase-field model of three-phase fluid flow system, *Comput. Methods Appl. Mech. Eng.*, **389** (2022), 114376. https://doi.org/10.1016/j.cma.2021.114376
30. I. Podlubny, *Fractional Differential Equations*, Academic Press, San Diego, 1999.
31. X. J. Li, C. J. Xu, A space-time spectral method for the time fractional diffusion equation, *SIAM J. Numer. Anal.*, **47** (2009), 2108–2131. https://doi.org/10.1137/080718942
32. J. L. Lions, E. Magenes, *Non-Homogeneous Boundary Value Problems and Applications*, Springer-Verlag, Berlin, 1972.
33. P. Grisvard, *Elliptic Problems in Nonsmooth Domains*, SIAM, Philadelphia, 2011. https://doi.org/10.1137/1.9781611972030
34. H. Triebel, *Interpolation Theory, Function Spaces, Differential Operators*, North-Holland Publishing Company, Amsterdam, 1978.
35. Z. P. Mao, S. Chen, J. Shen, Efficient and accurate spectral method using generalized Jacobi functions for solving riesz fractional differential equations, *Appl. Numer. Math.*, **106** (2016), 165–181. https://doi.org/10.1016/j.apnum.2016.04.002

AIMS Press